Chapter

An Efficient Approach Based on the Near-Field Technique to Solve EMI Problems: Application to an AC/DC Flyback Converter

Bessem Zitouna and Jaleleddine Ben Hadj Slama

Abstract

Flyback converters have been widely used in low- and high-power applications because of their simplicity and low cost. However, they incur electromagnetic compatibility problems which are more difficult to control. The present chapter proposes an efficient modeling method based on the near-field technique to solve real-world radiation problems of the power electronics circuits. Firstly, for the characterization of an AC/DC flyback converter, several experimental measurements of the magnetic near field are performed in the time domain over the converter. Subsequently, we have applied the time domain electromagnetic inverse method based on the genetic algorithms on the measured signals to find the equivalent radiating sources of the studied circuit. The accuracy and the efficiency of the proposed approach have been demonstrated by the good agreement between cartographies of the near magnetic field components calculated using the developed model and those measured. Finally, the developed equivalent model has been used to predict cartographies of other components of the magnetic field which will be compared to measured cartographies. This confirms that the identified equivalent sources can represent real sources in the studied structure. The proposed method could be used for diagnosis and fault location in power electronics systems.

Keywords: electromagnetic compatibility (EMC), flyback converter, inverse method, near-field measurement, time-domain analysis, genetic algorithms

1. Introduction

To respond to the necessity and simplicity of marketed converter applications, innovation in power electronics is based on the growing constraints imposed by the exponential rise of our needs: better management of primary energy sources while offering increasingly sophisticated functions at reduced cost. This cost function can obviously take different forms depending on the context: weight, volume, efficiency, disturbances on the converter and its environment, technological cost, economic cost, protection and reliability, and lifetime of devices. No device can be excluded today from environmental constraints. At this stage, a lot of energy conversion structures are now very efficient. For example, the flyback converter is probably the most widely used structure in the electronics industry and is

frequently utilized for various applications (battery chargers, energy saving lamps, photovoltaic systems, LCD monitors, DVD players, ...). Integration and coexistence in the same housing, as well as the increase in switching frequencies and carried powers, cause frequent and unwanted electromagnetic interference in the vicinity of these systems. These interferences present important sources of malfunction of the device itself and neighboring systems. For this reason, electro-magnetic compatibility (EMC) must be addressed from the starting process of design and manufacture of high-tech electronic devices. Indeed, the study of electromagnetic compatibility of a card gives quantitative tools to the power electronics to influence the radiated and conducted disturbances. It is essential to know the electromagnetic disturbances emitted by the equipment under test at different distances and to verify that they do not exceed a certain limit in order to avoid disturbing the neighboring equipment. Therefore, the EMC characterization tests have become an essential step in the various phases of the development of power electronics products. Unfortunately, these tests remain costly because we often need heavy, precise and very expensive equipment (anechoic chamber). To circumvent these limits, it is essential to develop radiating models that allow us to estimate the electromagnetic emissions of these systems before the prototype is realized (during the phase of virtual prototyping). The objective of this work is to elicit the electromagnetic inverse method in the time domain based on the near-field technique as an innovative and important solution that allows characterizing and modeling the radiation of the products of the power electronics. Thus, the added value of this chapter is to show the implementation of the inverse electromagnetic method in the time domain for the field of power electronics. In fact, the proposed approach will be of some use to people who make the development of power electronics systems. Actually, identifying all the sources of radiation in an electronic cartography and developing an equivalent radiation model that will allow us to estimate the electromagnetic emissions of these systems help solve the problems of interferences encountered in power electronics. The proposed method can be used for example as a method of analysis, fault detection and diagnosis of power electronic circuits. Indeed, the electromagnetic signature of a component could make it possible to verify its proper functioning. In order to find solutions related to the problems encountered in power electronics, the inverse electromagnetic method has been applied to different types of circuits.

In the literature, a lot of work has been already achieved on the modeling of electronic components [1–3]. The inverse method based on the elementary dipoles was used to extract the equivalent model from PCB circuits [4–6]. In frequency domain, the inverse method was also used in order to model electronics cards [7–9].

These various approaches have been developed in the frequency domain and have been utilized to characterize and to model the radiated emissions on only one frequency. It seems that there is no time. This supposes that the studied systems have had sinusoidal radiations that do not correspond to the reality of power electronic systems where the electromagnetic disturbances are very important over a broad band of frequencies. For this effect, modeling this kind of radiation by the frequency inverse method requires to repeating the identification of equivalent sources for each signal frequency. This causes a very high processing time. However, from the results found in the frequency domain, we cannot know at what time of the cycle of operation the radiating sources intervene, and we thus suppose that the radiations of the sources contribute simultaneously, which does not correspond to reality. Nevertheless, the switching in power electronics often presents offsets which will be found at the level of radiated emissions. The spectral distribution therefore evolves as a function of time and the components do not all have the same

radiation frequencies. Consequently, the models obtained by the electromagnetic inverse method in the frequency domain have several limitations and remain inapplicable for power electronics systems which are excited by different types of nonsinusoidal signals and which consequently emit on one broad band of frequencies. To this end, the added value of our approach is to propose an efficient technique based on the inverse electromagnetic method in the time domain which takes into account the temporal offset at the levels of the various radiated emissions of the circuit, which permits the Identification of the contribution of each radiating source of the circuit over time.

Until now, few studies have been performed and published on the time-domain inverse method. The authors in some study tried to combine the frequency inverse method with the time-frequency computation method [10, 11]. However, the developed modeling method was limited because it always depended on the parameters of the time intervals that mainly depended on the selected frequency band, the considered initial frequency and the used computer performance. Other approaches have been performed [12–15]. These studies were dedicated to the development of new computational techniques and analysis of an electromagnetic near field in the time domain. To develop a resolution method in the time domain, enabled by passing this kind of problem, we put forward the development and implementation of the temporal inverse electromagnetic method based on elementary dipoles [16].

The methodology of the time-domain electromagnetic inverse method has been presented [16]. This method was applied to identify the equivalent radiation model in a fairly simple structure, which was unfortunately not representative enough for all power electronic circuits. To demonstrate again the robustness and efficiency of the electromagnetic inverse method developed in the time domain when applied to complicated real cards composed of several bulky components, where the radiating sources are usually very close to each other, we propose to study in this chapter a complete application case (PCB and power electronic components). Hence, we will focus much more on the application of the temporal inverse electromagnetic method to find an equivalent model of an industrial system that emits nonsinusoidal radiations. This will make it possible to calculate the field emitted by the studied system for various distances and to study the coupling with the neighboring systems.

In this chapter, the time domain electromagnetic inverse method is tested and used in an AC-DC flyback converter application. First, we describe the device under test. Then, we will present how the suggested approach is implemented and what these advantages can be. To do this, several works will be performed. We will firstly present the test bench of the near field in the time domain. Second, we will present the measurement results of the vertical component of the radiated magnetic near field (H_z) performed over an AC/DC converter, so as to model the radiation of this converter by the electromagnetic inverse method in the time domain. In the following part, the modeling methodology and its resolution based on the genetic algorithms are described. To validate the identified model using our suggested approach, a comparison is made between the tangential components (H_x) of the magnetic field, calculated using the optimized model parameters and the one measured over the studied converter.

2. Description of the studied flyback converter

The system studied in this chapter is an AC-DC converter based on the principle of switched-mode power supplies (**Figure 1**).

Switching power supplies are much smaller and lighter than linear power supplies, which explain their increasingly widespread use in various fields, particularly in those of embedded systems. Also, switched-mode power supplies have a good efficiency until 90%. Contrarily, they have regulatory problems which are more difficult to control [17–19]. Due to the rectangular signal to the switching frequency, these power supplies produce a relatively large noise. This problem makes them unsuitable for certain applications. To this end, it is essential to characterize and control the EMC behavior of this type of converters.

The studied converter in this chapter is of a flyback type of a low power (5 W). The basic schema of a studied converter is illustrated in **Figure 2**.

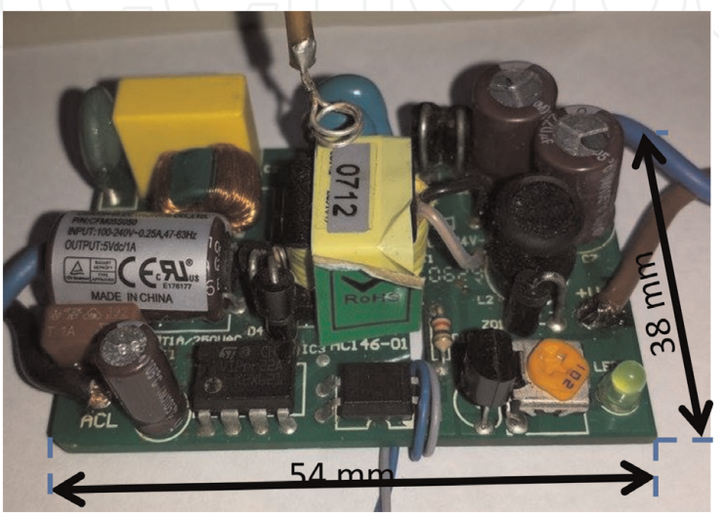

Figure 1.
Flyback AC/DC converter.

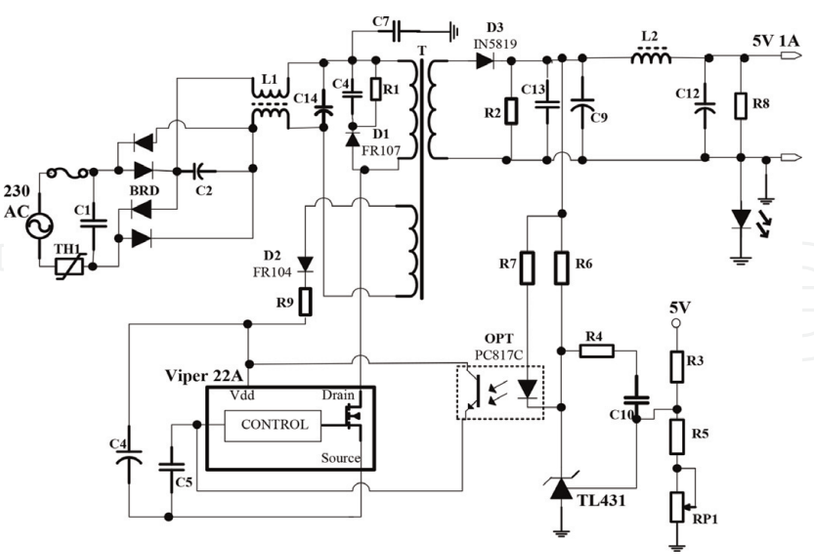

Figure 2.
Schematic of AC/DC flyback converter.

Type	Input voltage	Output voltage	Maximum current	Efficiency
Flyback	220 V AC	5 V DC	1 A	79%

Table 1.
Characteristics of studied converter.

The electrical characteristics of the studied flyback converter are illustrated in **Table 1**.

3. Description of magnetic near-field test bench in time domain

In our study, the measurement of the studied converter radiation is carried out in one single measurement for different radiation frequencies. This presents the benefits of a near field in the time domain compared to the frequency test bench.

Figure 3 presents the different parts of the near-field test bench in time domain.

The temporal measurement method uses a high-precision oscilloscope that presents a wide bandwidth. This oscilloscope is utilized for displaying and recording temporal signals picked up by the measurement of the magnetic field probe.

To sweep the probe above the studied structure, a plotting table is used. The displacement of the probe over the device under test is manually performed (**Figure 4**).

The displacement of the probe above the studied structure is manually performed. The displacement procedure of the probe from measurement point to another on the sweeping surface is described in **Figure 5**.

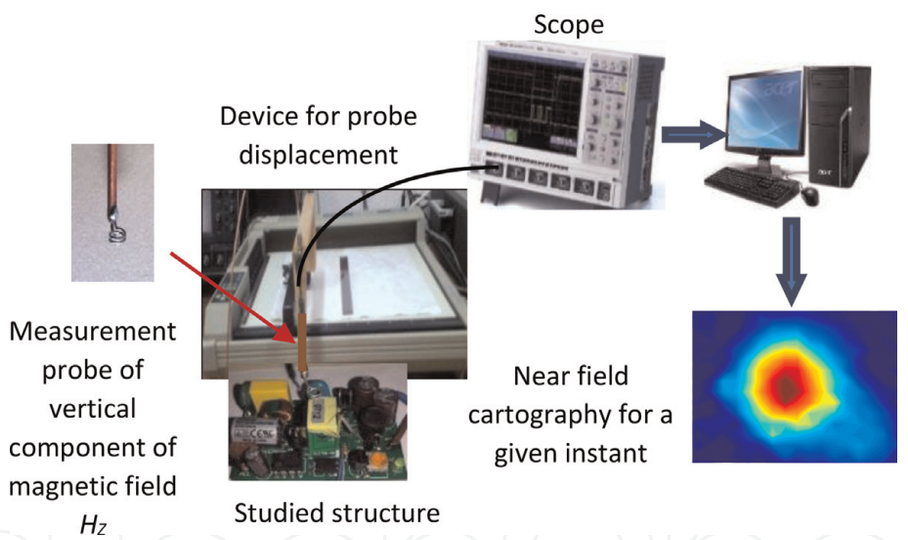

Figure 3.
Near-field test bench in time domain.

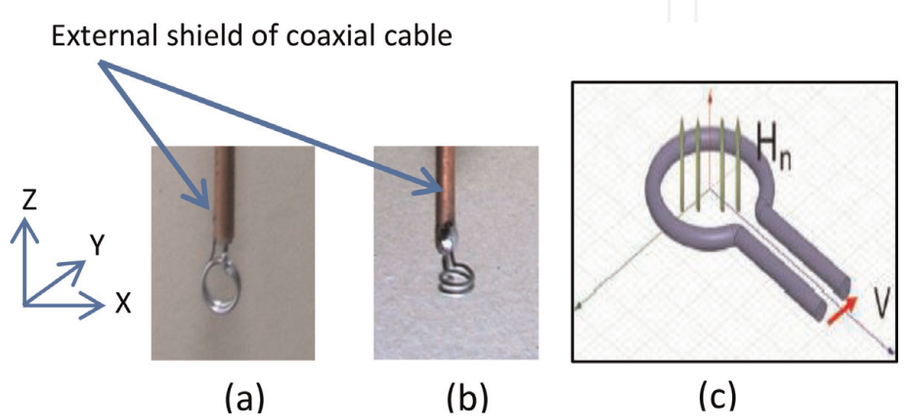

Figure 4.
Detailed structure of magnetic probes: (a) probe of tangential components H_x and H_y, (b) probe of vertical component, (c) measurement principle of electronic probe H_z.

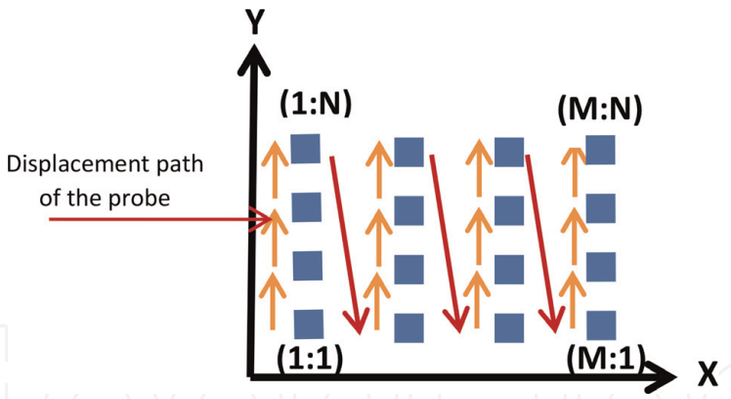

Figure 5.
Probe displacement in measurement surface.

In this study and according to our needs, we utilize two coil probes: one for measuring the normal component of the magnetic field (H_z) and the other for measuring the two tangential components (H_x and H_y). Each utilized probe is shielded. The shielding of the used probe is made by copper. It consists of a loop connected to the central conductor on one side and to the external shield of a coaxial cable on the other side, as shown in **Figure 4**. The probe is connected to the oscilloscope through a highly shielded coaxial cable.

To measure the magnetic fields around the components and systems, we use magnetic probes; and to capture the different components of the magnetic field H, it is necessary to place the normal to the surface of the collinearly loop of the desired component. It is possible to utilize a single probe and to orient it differently according to the component to be measured. The principle of the measurement protocol is based on the Faraday and Lenz law, which stipulates that if a variable magnetic field crosses through a closed circuit, then the resulting flux variation will cause an electromotive force at the terminals of the loop (**Figure 4c**). Accordingly, we have:

$$e(t) = -\frac{d\varphi(t)}{dt} \tag{1}$$

Finally, and through a transformation equation, we can deduce the magnetic field. The magnetic probe allows transforming the variable magnetic flux which crosses through it into a voltage at its terminals. Subsequently, we deduce the magnetic field at the center of the probe. Indeed, for a circular conductive loop of a radius R dived in a magnetic field B(t), the induced potential difference by the variable magnetic field is given by the following equation:

$$V(t) = -\oint \mu_0 \frac{\partial H(t)}{\partial t} \ \vec{\mathrm{n}} \ dS \tag{2}$$

where $\vec{\mathrm{n}}$ is the probe surface normal.

Since the probe surface is small enough, we can consider the magnetic field $H_z(t)$ constant over the entire loop area S. As a result, Eq. (5) becomes:

$$V(t) = -\mu_0 \times S \frac{\partial H(t)}{\partial t} \tag{3}$$

where $S = \pi \times r^2$ is the probe surface (r = 1.6 mm) and $\mu_0 = 4 \times \pi \times 10^{-7}$ H/m is the permeability in the free space.

In fact, extracting the magnetic field H(t) from the measured voltage at the probe terminals can be defined as follows:

$$H(t) = -\frac{1}{\mu_0 \times S}\int_0^t V(t)\ dt \tag{4}$$

4. Measurement of near field emitted by studied converter

This suggested approach is based on time domain measurements of the near field above the studied structure. The distribution of the near field on the chosen scanned surface is presented in the form of cartography. The cartography is a matrix representation of the amplitude and the phase of the measured near field at each point and at each instant over the studied system. It is characterized by the dimensions of the measurement surface (Xmin:Xmax; Ymin:Ymax), the distance between two measuring points (ΔX et ΔY), and the measuring height (Z) (**Figure 6**).

Figure 7b represents the chosen face used for the time domain measurements to identify the equivalent radiating sources. This face enables a good detection of the magnetic near field radiated by all components of the studied card.

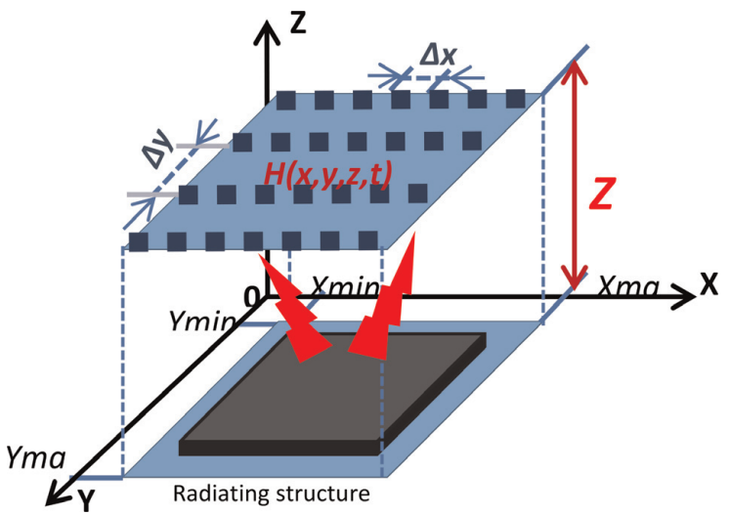

Figure 6.
Cartography parameters of near-field measurements.

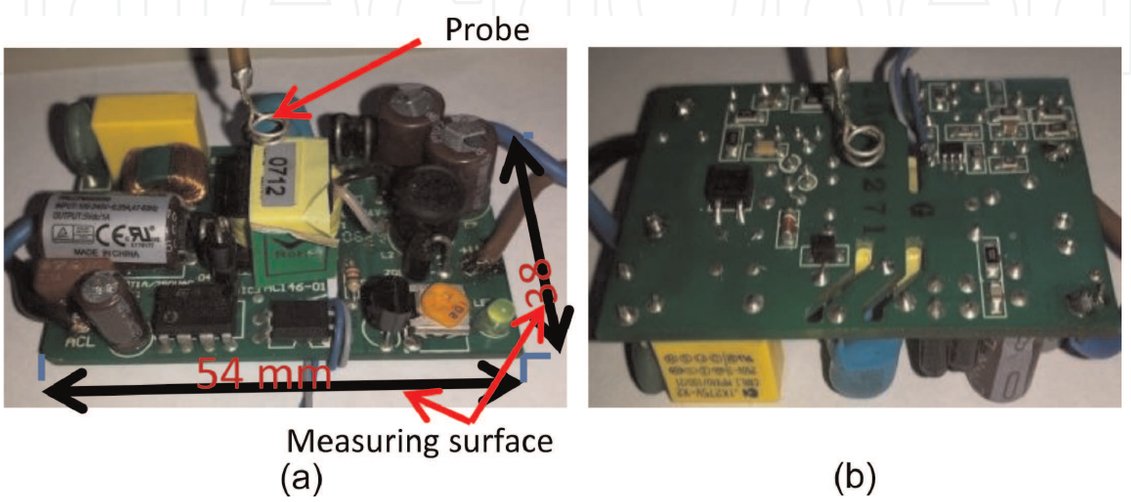

Figure 7.
(a) The studied card and (b) the selected studied card face for measuring the magnetic near field used to identify the model.

By analogy with the frequency inverse method, in this work, the identification of the equivalent radiating sources is based on the measurements of the magnetic near field [8, 9, 20]. This demonstrates its effectiveness in guaranteeing the uniqueness of the equivalent radiating model [9]. To bypass the complexities to measure the electrical near field, it is possible to extract the values of the electric field by exploiting the measurements of the magnetic field [21, 22].

5. Equivalent radiating model of studied flyback converter

In this study, the proposed temporal electromagnetic inverse method is based on the genetic algorithms. To apply our approach, a near-field measurements characterized by a very high signal-to-noise ratio are needed. The proposed method consists in identifying an equivalent model that emits the same radiation of the studied structure to be modeled.

The optimized equivalent model is based on a network of electric or magnetic dipoles (**Figure 8**).

The dipole may be represented by a d vector that comprises all the parameters: $d = (M_d, x_d, y_d, z_d, \theta_d, \varphi_d)$, where M_d is the magnetic moment of the dipole which varies against time. The x_d, y_d and z_d represent the dipole's position, and their orientations are represented by θ_d and φ_d. In the time domain, the components of the magnetic field emitted by the elementary electric and magnetic dipoles in an observation point M (x_o, y_o, z_o) can be deduced from the analytical expressions in the frequency domain using the frequency-time transformation operator. In the Cartesian coordinate system, the magnetic field components are expressed by the following equations [16]:

For the electric dipole:

$$\begin{bmatrix} H_x \\ H_y \\ H_z \end{bmatrix} = -\frac{\Delta l}{4\pi R^2} \times \left(\frac{1}{c}\frac{dI(t')}{dt} + \frac{1}{R} I(t') \right) \left(\begin{bmatrix} \sin\theta & \sin\phi \\ \sin\theta & \cos\phi \\ \cos\theta & \end{bmatrix} \cdot \begin{bmatrix} xd - x0 \\ yd - y0 \\ zd - z0 \end{bmatrix} \right) \wedge \begin{bmatrix} xd - x0 \\ yd - y0 \\ zd - z0 \end{bmatrix} \begin{pmatrix} \vec{i} \\ \vec{j} \\ \vec{k} \end{pmatrix} \tag{5}$$

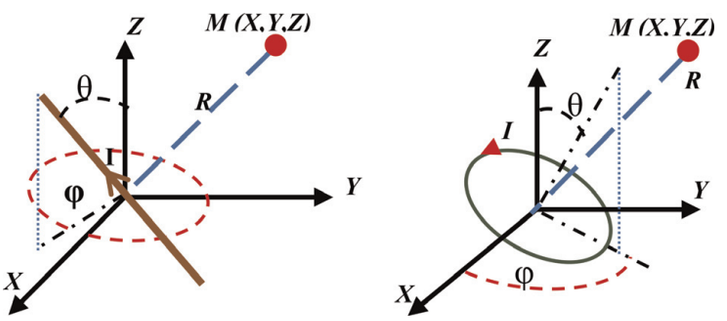

Figure 8.
Presentation of the elementary dipoles.

For the magnetic dipole:

$$\begin{bmatrix} H_x \\ H_y \\ H_z \end{bmatrix} = -\frac{r^2}{4R} \times \left[\left(\frac{1}{c^2} \frac{d^2 I(t')}{dt^2} + \frac{1}{Rc} \frac{dI(t')}{dt} + \frac{1}{R^2} I(t') \right) \begin{bmatrix} \sin\theta & \sin\phi \\ \sin\theta & \cos\phi \\ \cos\theta & \end{bmatrix} - \frac{1}{R^2} \left(\frac{1}{c^2} \frac{d^2 I(t')}{dt^2} + \frac{3}{Rc} \frac{dI(t')}{dt} + \frac{3}{R^2} I(t') \right) \left(\begin{bmatrix} \sin\theta & \sin\phi \\ \sin\theta & \cos\phi \\ \cos\theta & \end{bmatrix} . \begin{bmatrix} xd - x0 \\ yd - y0 \\ zd - z0 \end{bmatrix} \right) \wedge \begin{bmatrix} xd - x0 \\ yd - y0 \\ zd - z0 \end{bmatrix} \begin{pmatrix} \vec{i} \\ \vec{j} \\ \vec{k} \end{pmatrix} \right] \tag{6}$$

where $R = \sqrt{tt'??(Xd - Xo)^2 + (Yd - Yo)^2 + (Zd - Zo)^2}$ t′ = t − (R/c) is the delay time variable, $R = \sqrt{(Xd - X0)^2 + (Yd - Y0)^2 + (Zd - Z0)^2}$.

As the temporal measured signals above the studied system are not sinusoidal well as the excitations currents are not unique. In this proposed method, it is not necessary to initially propose a number of elementary dipoles during the equivalent model identification. Thus, the proposed method consists in identifying at each time a single particular dipole, until the identification of all dipoles that corresponds the equivalent model. Because the measures are performed at a very close distance above the studied structure, a hypothesis is adopted; it is based on the linearity between the radiated magnetic field by an elementary dipole and the current flowing in this dipole. This assumption is adopted for guessing the currents forms on the various dipoles, and is very helpful when simplifying the resolution during the optimization phase of the equivalent model parameters by the genetic algorithms.

At this stage, the problem of identifying the source dipoles is processed. The identification procedure of the radiating sources is presented in the following flowchart given in **Figure 9**.

In order to identify accurately the shape of the first dipole excitation signal, we will apply to the initially measured cartography a subprogram to seek the measured signal which has the maximum amplitude relative to other measured maximum temporal signals in this cartography. And on the basis of the measurement point that corresponds to the most intense radiation, we extract a limited part of the initial cartography and we propose a single elementary radiating dipole (electric or magnetic dipole) for the extracted cartography. In fact, the searched current form flowing in the first dipole to identify is well known; it is a normalized temporal signal relative to this measured maximum signal in this local cartography. Subsequently, an optimization method based on the genetic algorithms is applied to identify the parameters of the proposed dipole in this selected cartography. At each iteration, the genetic algorithms shall modify all the parameters of the dipole (a constant k which represents the amplitude of the excitation current circulating in

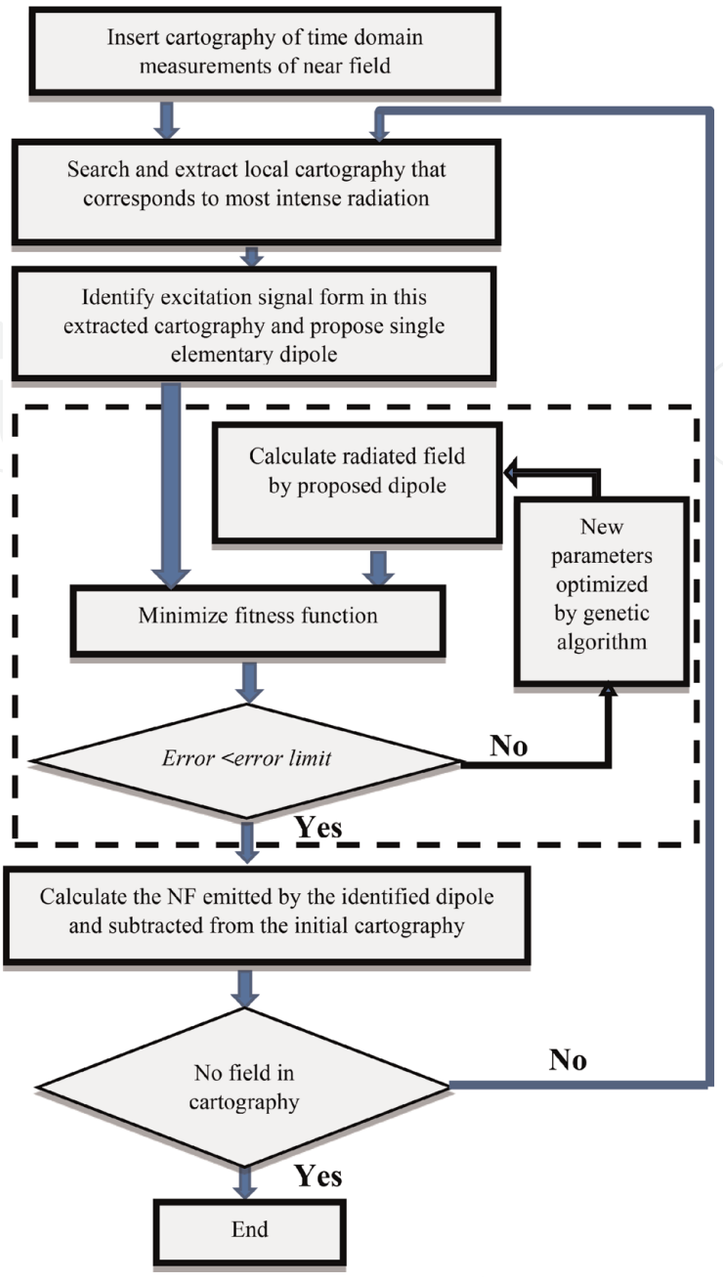

Figure 9.
Chart of proposed method based on optimization algorithm.

this proposed dipole, its geometry, its coordinates, and its orientations) in order to minimize the error calculated by the fitness function. If the error is unacceptable and the genetic algorithms cannot converge after a certain number of iterations, the optimization cycle repeats itself several times until obtaining a new composed generation of best solutions who is the calculated field coincides with the measured one on all points of the cartography and at all moments (even in the case of the small values of the measured field). Thus, the radiating dipole and its corresponding parameters are identified.

By using the analytical equations, the parameters of the first identified dipole are used to calculate the near magnetic field radiated in order to delete it from the initial measured cartography. This simplifies the resolution of the remaining cartography. The procedure is repeated until the scanning of all the measured cartography and the different dipole sources are identified.

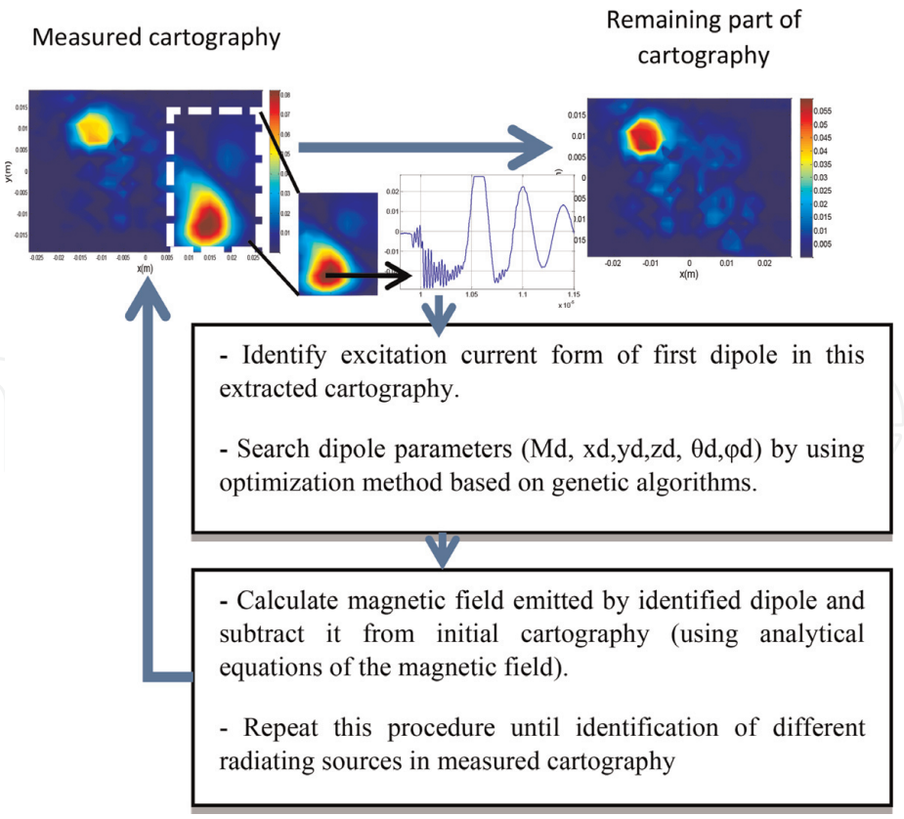

Figure 10.
Methodology of proposed electromagnetic inverse method in time domain.

Fitness function	$Error = \sum_{t_K=1}^{T} \sum_{i=1}^{M} \left\| \frac{H_Z(i, t_K)\text{measured-}H_Z(i, t_K)\text{estimated}}{H_Z(i, t_K)\text{measured}} \right\| \times 100$
Population size (N_p)	$N_p = 20 \times$ number of parameters of dipoles
Selection function	Roulette
Crossover rate	0.8

Table 2.
Optimum parameters of genetic algorithms.

A supplementary explanation of the proposed approach is illustrated in **Figure 10**. At each identification, this procedure will be repeated until the extraction of all radiating sources in this measured magnetic fields cartography.

The superposition method is applied in a near-field zone where it is assumed that in each area of the local cartography we identify a relatively intense field. The emission is mainly caused by a very close source and the contributions from the other relatively distant sources are very low compared with that of the intense source. Consequently, the search for the model is carried out dipole by dipole until identifying all radiating sources in the initially measured cartography. Indeed, the fitness function is used by the genetic algorithms for identifying the existing source in the each local cartography. Thus, the error of the global cartography is the sum of the errors of different local cartographies.

To guarantee and accelerate the convergence of the proposed temporal inverse method, we take into account the study of [23] to choose the optimal parameters of the genetic algorithms. These parameters are given in **Table 2**.

By applying the proposed method to identify the radiating sources, we have found seven magnetic dipoles as a number of sources. Despite the high density of

components in the converter and knowing that the measurements of radiated disturbances are performed at a very close distance above these components, and on the basis of research work on the modeling of the radiation of electronic components and systems, we have carried out the analysis of the radiations of the studied converter. This permits us to identify the original components of the equivalent radiating dipoles. Unfortunately, the modeling of systems by the inverse method in the frequency domain has several limitations and remains not applicable for systems of power electronics operating over a wide frequency band and excited by different types of nonsinusoidal signals. At this stage, it is the interest of the temporal inverse method proposed in this chapter. Thus, without modeling of the radiated emissions for each frequency of the measured signals (which causes a very significant calculation time). The proposed approach has the advantage of finding

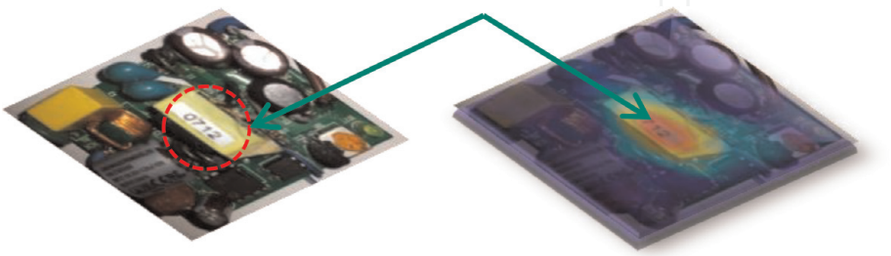

Figure 11.
Equivalent radiating source of transformer determined by proposed method.

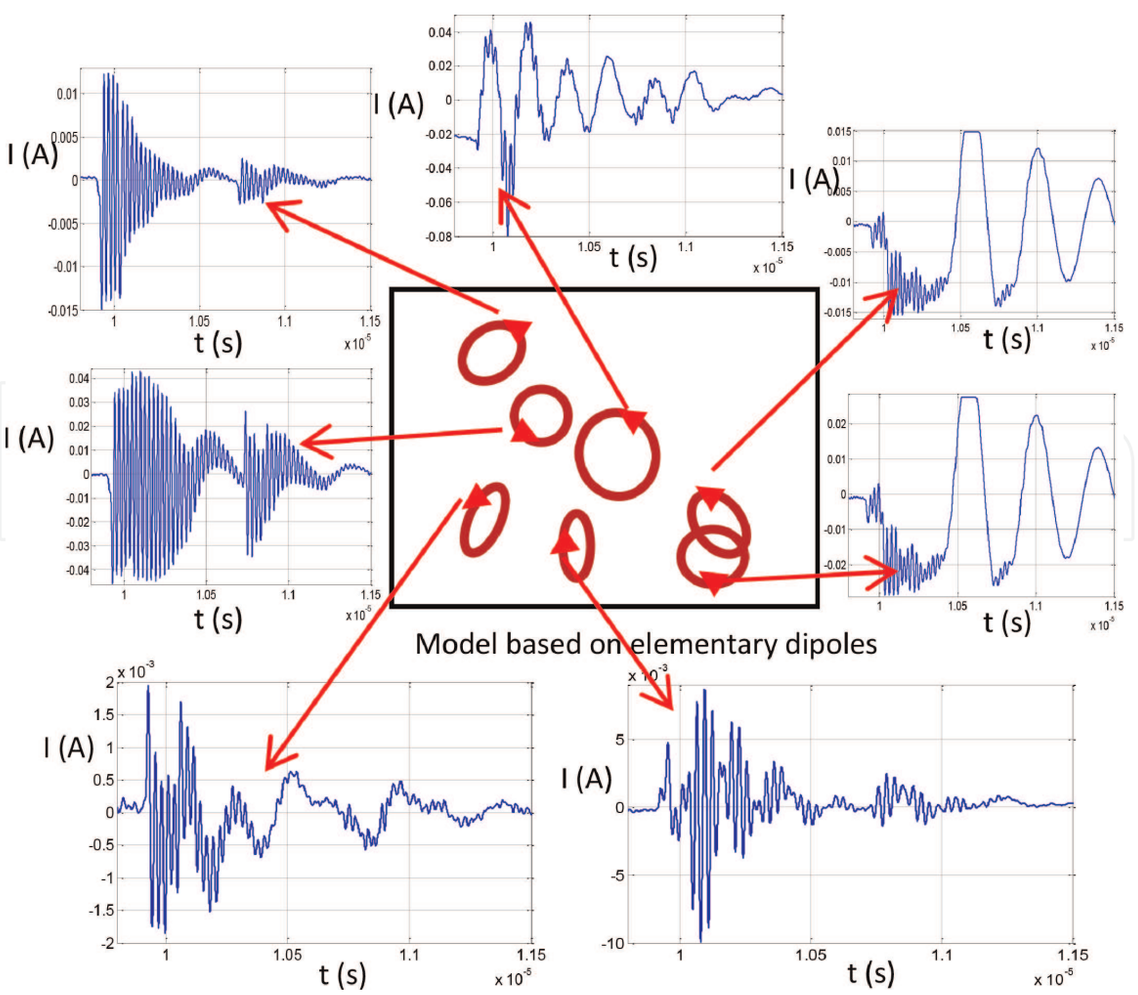

Figure 12.
Identified equivalent model of studied structure and forms of excitation signals.

in a reasonable processing time a single model of radiation valid over the whole band of frequencies in measured signal. From the results obtained by the inverse method proposed in the time domain, we can see that the first two identified magnetic dipoles represent the equivalent models of two diodes. The third identified source represents the equivalent radiation of the transformer. In fact, this last source has a center situated at coordinates X_d = 0.10 cm, Y_d = −0.21 cm and Z_d = −1.21 cm of the studied structure. It presents the coordinates of the transformer position in the studied card, as depicted in **Figure 11**.

Figure 12 gives a spatial representation of the equivalent dipoles identified by our proposed approach as well as the different shapes of the excitation currents of the source dipoles.

The parameters of the equivalent model obtained by the proposed method are shown in **Table 3**.

Hence, it presents the case where the emitted disturbances of the tracks are very low compared to that of the components. Finally, we notice that the components of the power electronics card represent the majority of the radiation of the studied structure as illustrated in **Figure 13**.

In order to study these electromagnetic disturbances, we present in **Figure 14** the measured magnetic near-field cartographies at different moments.

Identified dipoles	M_{di} (A m^2)	[X_{di} Y_{di} Z_{di}] (cm)	$\theta_i(0)$	$\varphi_i(0)$
#1	3.12 e − 7	1.46/−1.33/−0.645	0.57	7.45
#2	4.42 e − 7	1.42/−0.32/−0.79	58.47	−132.99
#3	1.12 e − 6	0.10/−0.21/−1.21	9.17	9.74
#4	2.96 e − 7	−0.96/0.20/−0.61	−11.46	−17.77
#5	3.86 e − 7	−1.34/1.19/−0.65	−43.56	128.98
#6	1.48 e − 7	−0.35/−1.08/−0.37	72.80	179.42
#7	1.90 e − 8	−1.36/−0.74/−0.62	83.12	8.85

Table 3.
Model parameters obtained by the proposed method.

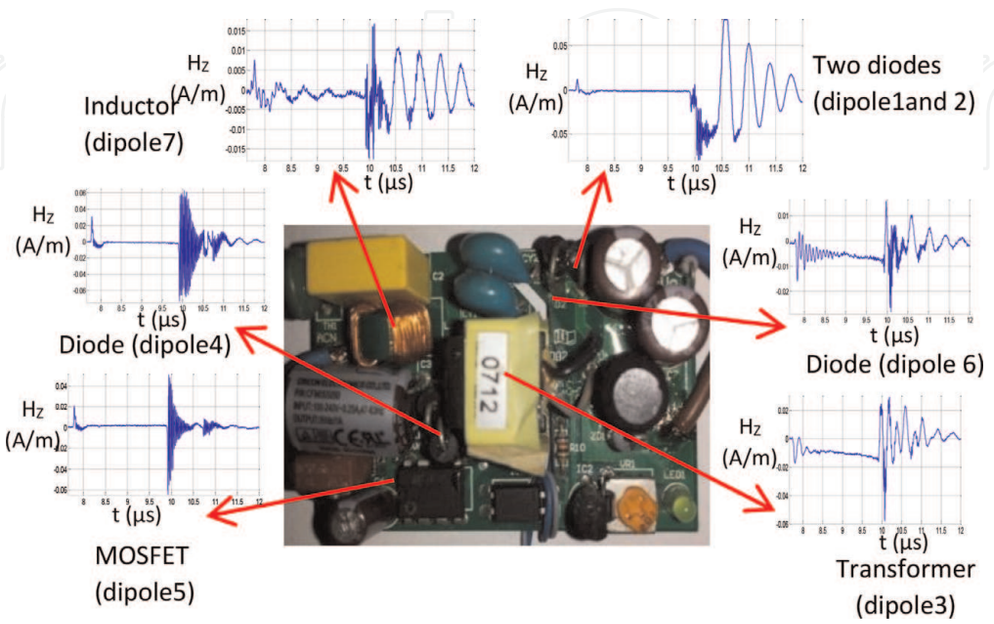

Figure 13.
Internal structure of studied converter and radiations emitted by different radiating components.

By analyzing **Figure 14**, we notice that the all sources do not appear at the same time. This is due to the time lag at the level of the electrical quantities passing through the different elements of the studied structure. This kind of transient phenomena is not easy to identify in the frequency analysis where the equivalent sources appear at the time such as presented in [8]. For a diagnostic study, where it is desired to control the good functioning of a sensitive element in a power electronics card, this type of time analysis becomes an effective alternative that enables

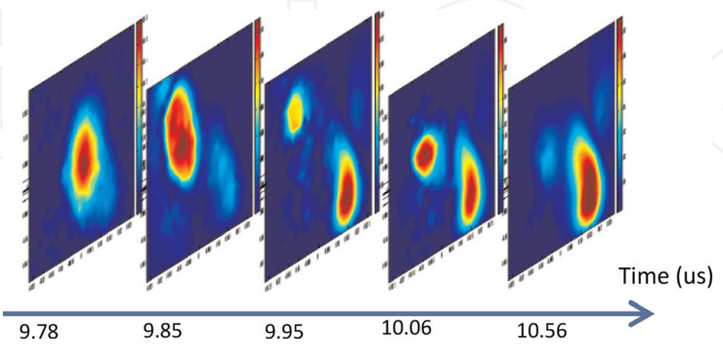

Figure 14.
Cartographies of the magnetic near field at various moments.

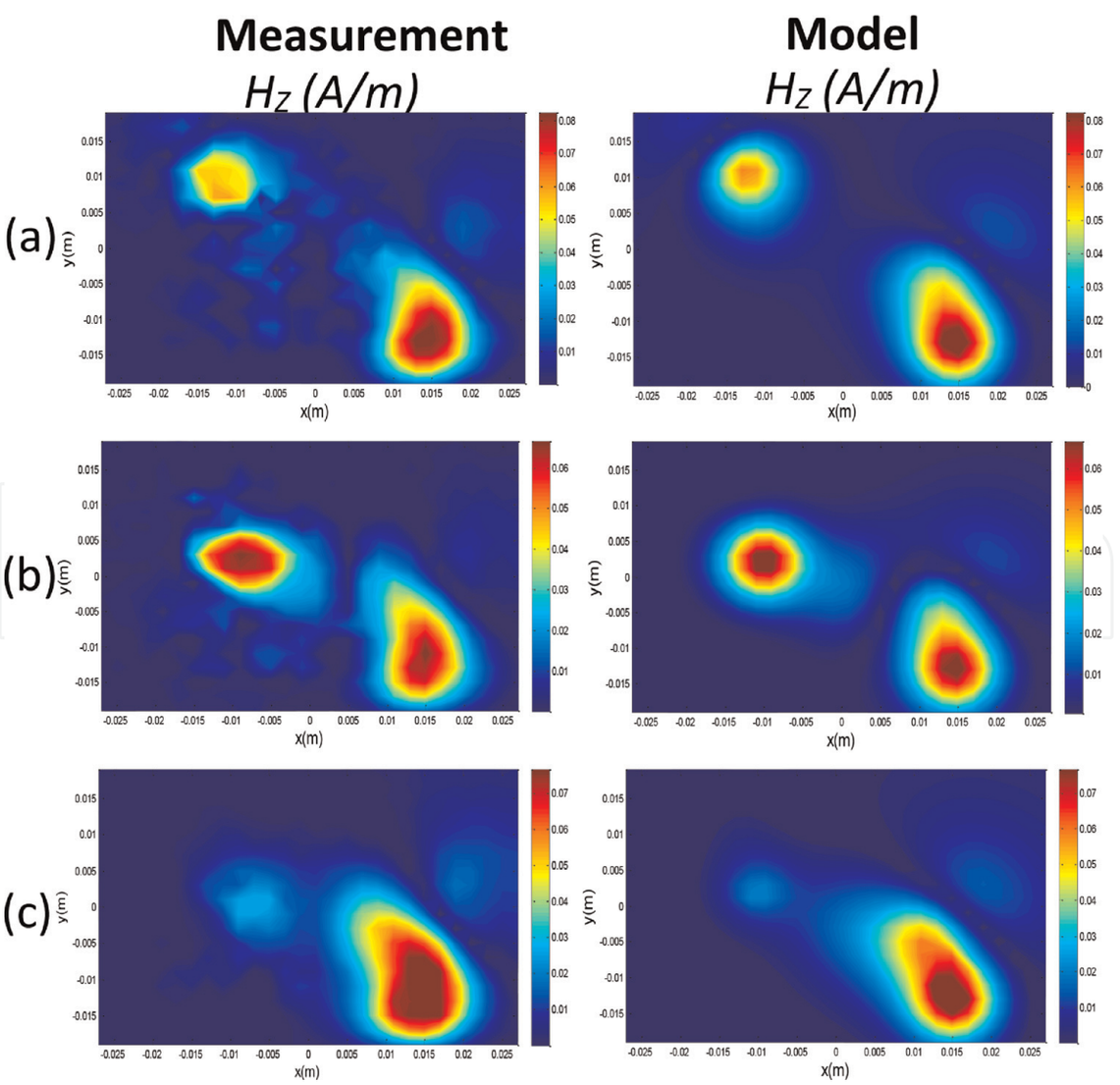

Figure 15.
Measured magnetic field and estimated one (a) t = 9.95 μs, (b) t = 10.06 μs, (c) t = 10.56 μs.

us to use the electromagnetic signature based on the temporal near field for the disgnosis of some components of the card. The electromagnetic inverse method in the time domain can therefore be used as a nonintrusive method of diagnosing and detecting defects in converter circuits. We cite for example the case of clamping-diode faults in a three-level NPC inverter circuit using the temporal analysis of the near magnetic field. Actually, the failure of a diode results in a modification during a delimited sequence at each period, from the temporal cartography of the magnetic field measured in a zone close to the circuit.

In **Figure 15**, we present at various moments a comparison between the measured cartographies of the normal magnetic field component (H_z) and the calculated cartographies using the parameters of the equivalent model obtained by the electromagnetic inverse method proposed in the time domain.

By examining the results got, we notice a good agreement between these cartographies. This demonstrates that the suggested method can identify with very good accuracy all radiating sources of the circuit.

6. Validation of identified equivalent model

In order to validate the found equivalent model, we measured the tangential component of the magnetic field (H_x measured) and subsequently we compared it with that is calculated (H_x estimated) by exploiting the optimized parameters of the

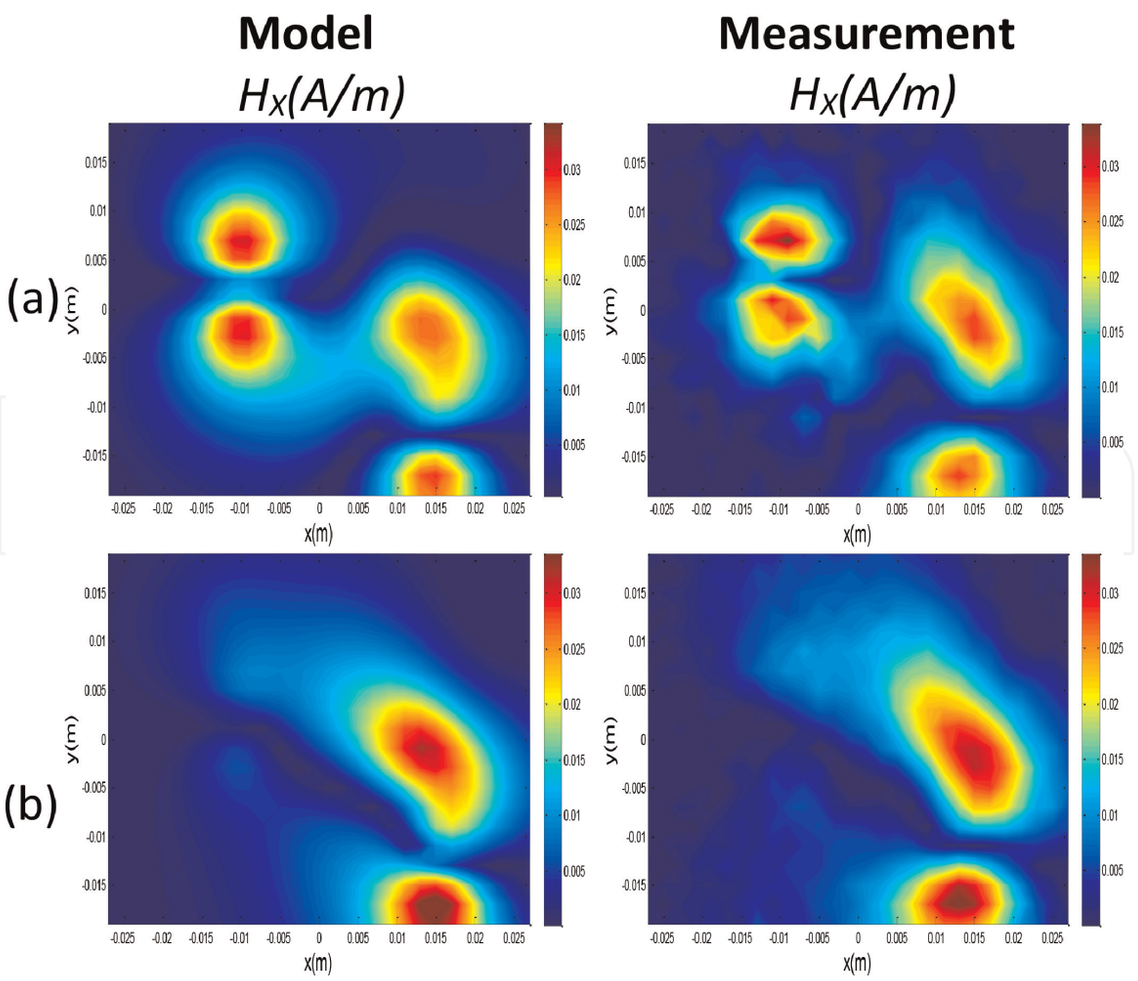

Figure 16.
Comparison of estimated near-field cartographies (H_x) to those measured at (a) t = 10.06 μs and (b) t = 10.47 μs.

equivalent radiating sources. In two distinct instants (t_1 = 10.06 μs and t_2 = 10.47 μs), a comparison between the measured and estimated of the near-field cartographies is presented in **Figure 16**.

According to the results presented in the previous figure, the magnetic near field calculated using the identified model parameters is in good agreement with the measured magnetic near field. These results confirm the existence of the equivalent sources network found by the electromagnetic inverse method in the time domain. Thus, the results showed that the proposed method guarantees the uniqueness of the solution. This confirms the effectiveness of the proposed approach for model the high-power structures where the radiated emissions are very high.

7. Conclusion

The frequency domain electromagnetic inverse method has several disadvantages when modeling radiation of power electronics systems. These disadvantages are mainly related to the radiation over a broad frequency band. To overcome these drawbacks, we have proposed in this chapter the use of the time domain electromagnetic inverse method. This novel method has been applied to identify the equivalent radiating sources of an AC-DC converter. The radiating sources are identified by exploiting the measurements of the vertical component (H_z) of the magnetic field performed over the studied converter. This equivalent model has been validated by using the measurements of the tangential component of the near magnetic field (H_x). The good agreement between the calculated results by using the optimized parameters of the equivalent model and the experimental results measured above the studied structure highlights the robustness of the suggested inverse problem when seeking equivalent radiating sources for industrial systems creating transient signals.

Author details

Bessem Zitouna* and Jaleleddine Ben Hadj Slama
Laboratory of Advanced Technology and Intelligent Systems (LATIS), National Engineering School of Sousse (ENISo), University of Sousse, Tunisia

*Address all correspondence to: bessem.zitouna@yahoo

References

[1] Saidi S, Ben Hadj Slama J. Analysis and modeling of power MOSFET radiation. Progress In Electromagnetics Research M. 2013;**31**:247-262

[2] Labiedh W, Ben Hadj Slama J. Analysis and modeling of the magnetic near fields emitted by an IGBT and by a power diode generic radiating model for active components. In: International Conference on Electrical Sciences and Technologies in Maghreb (CISTEM). 2014. pp. 1-6

[3] Levy P-E, Gautier C, Costa F, Revol B, Labarre C. Accurate modeling of radiated electromagnetic field by a coil with atoroidalferromagnetic core. IEEE Transactions on Electromagnetic Compatibility. 2013;**55**(5):825-833

[4] Shim HW, Hubing T. A closed-form expression for estimating radiated emissions from the power planes in a populated printed circuit board. IEEE Transactions on Electromagnetic Compatibility. 2006;**48**(1):74-81

[5] Tong X, Thomas DWP, Nothofer A, Sewell P, Christopoulos C. Modeling electromagnetic emissions from printed circuit boards in closed environments using equivalent dipoles. IEEE Transactions on Electromagnetic Compatibility. 2010;**52**(2):462-470

[6] Beghou L, Liu Y, Pichon L, Costa F. Synthesis of equivalent 3-D models from near field measurements application to the EMC of power printed circuits boards. IEEE Transactions on Magnetics. 2009;**45**(3):1650-1653

[7] Beghou L, Costa F, Pichon L. Detection of electromagnetic radiations sources at the switching time scale using an inverse problem-based resolution method—Application to power electronic circuits. IEEE Transactions on Electromagnetic Compatibility. 2015; **57**(1)

[8] Saidi S, Ben Hadj Slama J. A near-field technique based on PZMI, GA, and ANN: Application to power electronics systems. IEEE Transactions on Electromagnetic Compatibility. 2014; **56**(4):784-791

[9] Benyoubi F, Pichon L, Bensetti M, Le Bihan Y, Feliach M. An efficient method for modeling the magnetic field emissions of power electronic equipment from magnetic near field measurements. IEEE Transactions on Electromagnetic Compatibility. 2017; **59**(2):609-617

[10] Liu Y, Ravelo B, Fernandez-Lopez P. Modeling of magnetic near-field radiated by electronic devices disturbed by transient signals with complex form. Applied Physics Research. 2012;**4**(1): 3-18

[11] Liu Y, Ravelo B. Application of near-field emission processing for microwave circuits under ultra-short duration perturbations. Advanced Electromagnetics. 2012;**1**(3)

[12] Liu Y, Ravelo B. Fully time-domain scanning of EM near-field radiated by RF circuits. Progress In Electromagnetics Research B. 2014;**57**: 21-46

[13] Rioult J, Seethramdoo D, Heddebaut M. Novel electromagnetic field measuring instrument with real-time visualization. Proc IEEE Int. Symp. EMC, Austin, Texas, USA. 2009:133-138

[14] Ravelo B, Liu Y, Slama JBH. Time-domain planar near-field/near-field transform with PWS operations. The European Physical Journal Applied Physics. 2011;**53**(03):1-8

[15] Liu Y, Ravelo B, Jastrzebski AK, Hadj Slama JB. Calculation of the time domain z-component of the EM-near-field from the x- and y-components. In:

41st European Microwave Conference. 2011

[16] Zitouna B, Ben Hadj Slama J. Enhancement of time-domain electromagnetic inverse method for modeling circuits radiations. IEEE Transactions on Electromagnetic Compatibility. 2016;**58**(2):534-542

[17] Kim Y-H, Jang J-W, Shin S-C, Chung-Yuen W. Weighted-efficiency enhancement control for a photovoltaic AC module interleaved flyback inverter using a synchronous rectifier. IEEE Transactions on Power Electronics. 2014;**29**(12)

[18] Chen Y, Chang C, Yang P. A novel primary-side controlled universal-input AC-DC LED driver based on a source-driving control scheme. IEEE Transactions on Power Electronics. 2015;**30**(8)

[19] Zhu Z, Wu Q, Wang Z. Self-compensating OCP control scheme for primary-side controlled flyback AC/DC converters. IEEE Transactions on Power Electronics. 2017;**32**(5)

[20] Gao X, Fan J, Zhang Y, Kajbaf H, Pommerenke D. Far-field prediction using only magnetic near-field scanning for EMI test. IEEE Transactions on Electromagnetic Compatibility. 2014; **56**(6):1335-1343

[21] Ravelo B. E-field extraction from H-near-field in time-domain by using PWS method. Progress In Electromagnetics Research B. 2010;**25**:171-189

[22] Liu Y, Ravelo B, Jastrzebski AK. Calculation of time-domain near field $E_{x,y,z}(t)$ from $H_{x,y}(t)$ with PWS and FFT transforms. In: Proc. Int. Symp. Electromagn. Compat.; 17-20 September 2012; Roma, Italy. 2012. pp. 1-6

[23] Saidi S, Slama JBH. Effect of genetic algorithm parameters on convergence of the electromagnetic inverse method. In: 8th International Multi-Conference on Systems, Signals & Devices (SSD); 22-25 March 2011; Sousse, Tunisia. 2011. pp. 1-5